

Proceedings of the Fifth Annual LHCP
ATL-PHYS-PROC-2017-113
September 1, 2017

Monte Carlo modeling of Standard Model multi-boson production processes
for $\sqrt{s} = 13$ TeV ATLAS analyses

SHU LI

*On behalf of the ATLAS Collaboration,
Duke University, USA
Tsung-Dao Lee Institute, China
Shanghai Jiao Tong University, China*

ABSTRACT

Multi-boson production measurements provide an important test of the electroweak sector of the Standard Model. The production of multiple gauge bosons V ($= W^\pm, Z, \gamma$) opens up a multitude of potential decay channels categorized according to the number of charged leptons in the final state. We present the Monte Carlo setup used by ATLAS to model multi-boson processes in $\sqrt{s} = 13$ TeV proton-proton collisions. The baseline Monte Carlo generators are compared with each other in key kinematic distributions of the processes under study.

PRESENTED AT

The Fifth Annual Conference
on Large Hadron Collider Physics
Shanghai Jiao Tong University, Shanghai, China
May 15-20, 2017

ATL-PHYS-PROC-2017-113
01/09/2017



1 Motivation

In ATLAS experiment [1], the multiboson productions are ones of the most important processes for both Standard Model (SM) measurements (signals) and BSM searches (backgrounds). This study tries to investigate the performance of various benchmark generators used in ATLAS within the official software framework and provides a summary of such process modeling performances in ATLAS.

2 Generators

The following setups are used for the Monte Carlo (MC) simulation:

- List of Generators: **Sherpa** [2], **PowhegBox** [3, 4, 5], **MadGraph5_aMC@NLO** [6], **MC@NLO** [7], **VBFNLO** [8].
- List of Parton Shower (PS) setups: **PYTHIA8** [9], **HERWIG 7/HERWIG ++** [10], **Sherpa** [2].

The modeling of the multi-jet associations in the investigated processes are done with multi-leg matrix elements. The merging schemes being studied are CKKW, MEPS@NLO and FxFx depending on the generators [11].

3 Fully Leptonic diboson process modeling

The fully leptonic diboson processes are modeled by various generators at high precision as shown in Table 1.

Table 1: Overview of di-boson process accuracies for the generators. NLO: next-to-leading order, LO: leading order, PS: parton shower [11].

	$VV + 0j$	$VV + 1j$	$VV + 2j$	$VV + 3j$	$VV + \geq 4j$
Sherpa v2.2	NLO	NLO	LO	LO	PS
PowhegBox+PYTHIA8 /HERWIG++	NLO	LO	PS	PS	PS
MadGraph5_aMC@NLO +PYTHIA8	NLO	NLO	LO	PS	PS
MC@NLO +HERWIG	NLO	LO	PS	PS	PS

Figure 1 shows the kinematics comparisons between different generators and the data measurement in WZ production process and differential cross section predictions of **Sherpa** and **PowhegBox** in ZZ production process.

4 Electroweak diboson(+ jj) process modeling

The modeling of most electroweak diboson production processes in association with two jets is provided with LO precision for 2-jets and higher-jet multiplicities are modeled via parton showering. Only in the like-charged $W^\pm W^\pm \rightarrow \ell^\pm \ell^\pm 2\nu + jj$ process, **PowhegBox** provides NLO order modeling of 2-jet bin and leading order modeling 3-jet bin. At QCD LO without asking for vector boson decays, the electroweak (EWK) coupling order is 2 for QCD induced processes and 4 for EWK induced processes while the QCD coupling order is 2 for QCD induced processes and 0 for EWK induced processes. Figure 2 shows the opposite-charged $W^\pm W^\mp / ZZ \rightarrow \ell^\pm \ell^\mp 2\nu + jj$ process modeling comparison between **VBFNLO** and **MadGraph5_aMC@NLO**, and the like-charged $W^\pm W^\pm \rightarrow \ell^\pm \ell^\pm 2\nu + jj$ process modeling comparisons between different scale choices.

5 Triboson process modeling

The SM rare processes of triboson productions are modeled by **Sherpa** and **VBFNLO** at LO. **Sherpa v2.2** also provides NLO modeling of on-shell tribosons and LO modeling up to 2-jets. Higher jet multiplicities are modeled via parton showering. Table 2 summarizes the modeled precisions. Figure 3 shows the jet multiplicity and leading lepton p_T distribution comparisons between different generators.

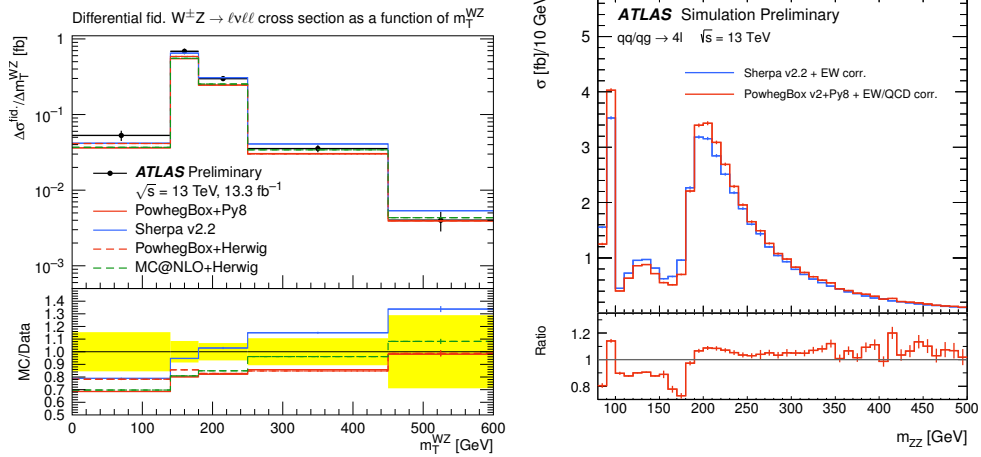


Figure 1: The modeled kinematics comparison between different generators in WZ and ZZ processes. The plot on the left shows comparison of differential $W^\pm Z$ cross section as a function of the transverse mass variable m_T^{WZ} for the $W^\pm Z$ system with PowhegBox + PYTHIA8, PowhegBox + HERWIG, Sherpa and MC@NLO + HERWIG predictions. The plot on the right shows the differential cross section predictions of Sherpa and PowhegBox both with higher-order electroweak effects and QCD effects corrections as the function of four-lepton invariant mass, which is rather insensitive to higher-order QCD effects according to the comparison [11].

Table 2: Overview of triboson process accuracies for the chosen generators [11].

	$VVV + 0j$	$VVV + 1j$	$VVV + 2j$	$VVV + \geq 3j$
VVV on-shell	Sherpa v2.2	NLO	LO	LO
$6\ell, 5\ell 1\nu, 4\ell 2\nu, 3\ell 3\nu, 2\ell 4\nu$	Sherpa v2.2	LO	LO	PS
$3\ell 3\nu$	VBFNLO+PYTHIA8	LO	PS	PS

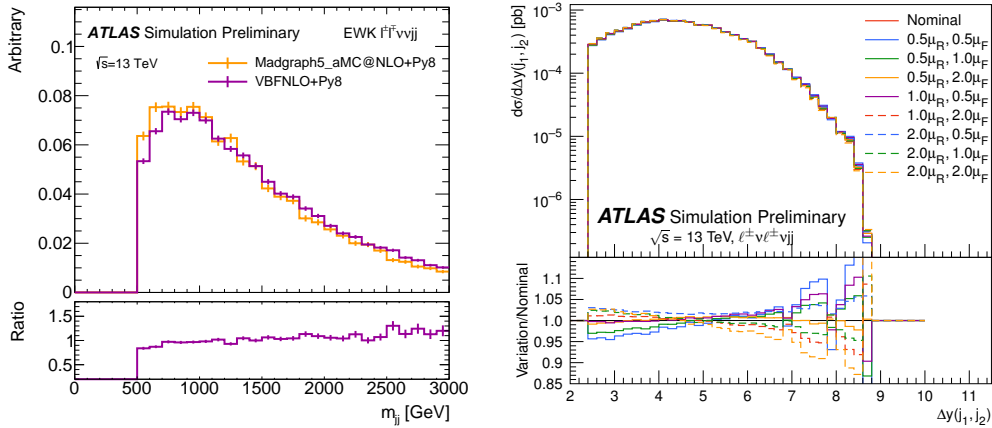


Figure 2: The modeled kinematics comparison between different generators in $W^\pm W^\mp / ZZ \rightarrow \ell^\pm \ell^\mp 2\nu + jj$ and with scale variations in $W^\pm W^\pm \rightarrow \ell^\pm \ell^\pm 2\nu + jj$ processes. The left plot shows in the $W^\pm W^\mp + jj$ channel the comparison of predicted kinematic distributions between MadGraph5_aMC@NLO and VBFNLO, both of which are showered with PYTHIA8, for di-jet invariant mass m_{jj} . The distributions is normalised to the same integral, and the shown uncertainties are statistical only. The right plot quantifies the impact of the scale variations on the rapidity separation $\Delta y(j_1, j_2)$ for the two leading jets [11].

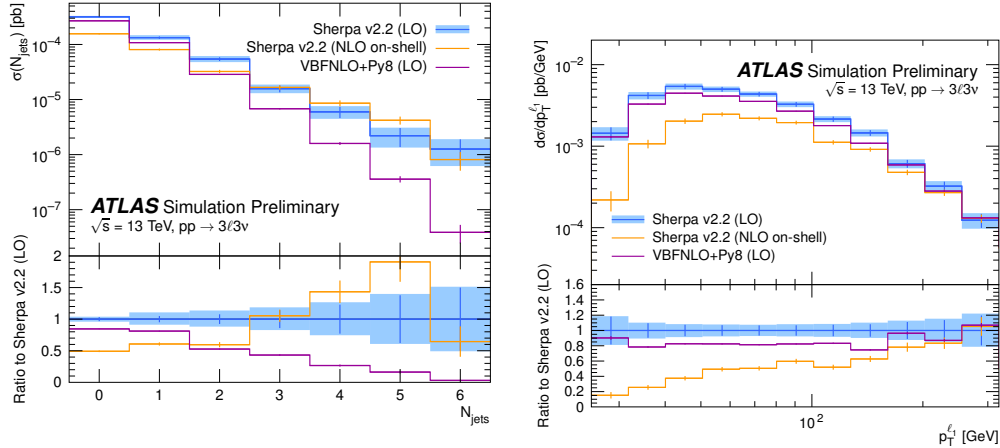


Figure 3: The modeled jet multiplicity and leading lepton p_T comparison between different generators in $WW \rightarrow 3\ell 3\nu$ process, in between Sherpa and VBFNLO [11].

6 Conclusion

We present the MC process modeling of multi-boson productions used by ATLAS at 13 TeV in pp collisions. State-of-the-art generators are investigated and key kinematic distributions of the processes are compared. Systematic uncertainties such as scale and PDF variations were also investigated and summarized in Ref. [11].

References

- [1] ATLAS Collaboration, “The ATLAS Experiment at the CERN Large Hadron Collider,” JINST 3 S08003 (2008).
- [2] T. Gleisberg et al., “Event generation with SHERPA 1.1,” JHEP 02 (2009) 007.
- [3] P. Nason, “A New method for combining NLO QCD with shower Monte,” JHEP 11 (2004) 040.
- [4] S. Frixione et al., “Matching NLO QCD computations with Parton Shower simulations: the POWHEG method,” JHEP 11 (2004) 040.
- [5] S. Alioli et al., “A general framework for implementing NLO calculations in shower Monte Carlo programs: the POWHEG BOX,” JHEP 06 (2010) 043.
- [6] J. Alwall et al., “The automated computation of tree-level and next-to-leading order differential cross sections, and their matching to parton shower simulations,” JHEP 07 (2014) 079.
- [7] S. Frixione et al., “Matching NLO QCD computations and parton shower simulations,” JHEP 06 (2002) 029.
- [8] J. Baglio et al., “Release Note - VBFNLO 2.7.0,” arXiv:1107.4038 [hep-ph].
- [9] T. Sjöstrand et al., “An Introduction to PYTHIA 8.2,” Comput. Phys. Commun. 191 (2015) 159.
- [10] J. Bellm et al., “Herwig 7.0 / Herwig++ 3.0 Release Note,” arXiv:1512.01178 [hep-ph].
- [11] ATLAS Collaboration, “Multi-Boson Simulation for 13 TeV ATLAS Analyses,” ATL-PHYS-PUB-2017-005, (<http://atlas.web.cern.ch/Atlas/GROUPS/PHYSICS/PUBNOTES/ATL-PHYS-PUB-2017-005/>)